






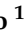



Article

Dynamic Mechanical Analysis and Ballistic Performance of Kenaf Fiber-Reinforced Epoxy Composites

Thuane Teixeira da Silva ^{1,*}, Pedro Henrique Poubel Mendonça da Silveira ¹,
André Ben-Hur da Silva Figueiredo ¹, Sérgio Neves Monteiro ¹, Matheus Pereira Ribeiro ¹,
Lucas de Mendonça Neuba ¹, Noan Tonini Simonassi ², Fabio da Costa Garcia Filho ¹,
and Lucio Fabio Cassiano Nascimento ¹

¹ Department of Materials Science, Military Institute of Engineering—IME, Praça General Tibúrcio 80, Urca, Rio de Janeiro 22290-270, Brazil

² Advanced Materials Laboratory (LAMAV), Department of Materials Engineering, State University of the Northern Rio de Janeiro—UENF, Avenida Alberto Lamego, 2000, Campos dos Goytacazes 28013-602, Brazil

* Correspondence: thuaneteixeiraa@gmail.com

Abstract: Several industry sectors have sought to develop materials that combine lightness, strength and cost-effectiveness. Natural lignocellulosic natural fibers have demonstrated to be efficient in replacing synthetic fibers, owing to several advantages such as costs 50% lower than that of synthetic fibers and promising mechanical specific properties. Polymeric matrix composites that use kenaf fibers as reinforcement have shown strength increases of over 600%. This work aims to evaluate the performance of epoxy matrix composites reinforced with kenaf fibers, by means of dynamic-mechanical analysis (DMA) and ballistic test. Through DMA, it was possible to obtain the curves of storage modulus (E'), loss modulus (E'') and damping factor, $\tan \delta$, of the composites. The variation of E' displayed an increase from 1540 MPa for the plain epoxy to 6550 MPa for the 30 vol.% kenaf fiber composites, which evidences the increase in viscoelastic stiffness of the composite. The increase in kenaf fiber content induced greater internal friction, resulting in superior E'' . The $\tan \delta$ was considerably reduced with increasing reinforcement fraction, indicating better interfacial adhesion between the fiber and the matrix. Ballistic tests against 0.22 caliber ammunition revealed similar performance in terms of both residual and limit velocities for plain epoxy and 30 vol.% kenaf fiber composites. These results confirm the use of kenaf fiber as a promising reinforcement of polymer composites for automotive parts and encourage its possible application as a ballistic armor component.

Keywords: kenaf fiber; dynamic-mechanical analysis (DMA); dynamic mechanical; epoxy composite; ballistic test



Citation: da Silva, T.T.; da Silveira, P.H.P.M.; Figueiredo, A.B.-H.d.S.; Monteiro, S.N.; Ribeiro, M.P.; Neuba, L.d.M.; Simonassi, N.T.; Garcia Filho, F.d.C.; Nascimento, L.F.C. Dynamic Mechanical Analysis and Ballistic Performance of Kenaf Fiber-Reinforced Epoxy Composites. *Polymers* **2022**, *14*, 3629. <https://doi.org/10.3390/polym14173629>

Academic Editor: Mariana Doina Banea

Received: 31 July 2022

Accepted: 26 August 2022

Published: 2 September 2022

Publisher's Note: MDPI stays neutral with regard to jurisdictional claims in published maps and institutional affiliations.



Copyright: © 2022 by the authors. Licensee MDPI, Basel, Switzerland. This article is an open access article distributed under the terms and conditions of the Creative Commons Attribution (CC BY) license (<https://creativecommons.org/licenses/by/4.0/>).

1. Introduction

Several industrial sectors, e.g., automotive and aeronautics, seek to develop lighter and more resistant materials as a way of increasing mechanical performance [1,2]. The composite materials, mainly those comprising a polymeric matrix reinforced with fibers, fit well in answering to these demands owing to their high stiffness capacity and strength improvement associated with lower density [3], as well as favorable cost-effectiveness. As a continuous demand effect, some alternatives to the broadly synthetic fibers, specially glass fibers, have recently been increasingly explored in view of even cheaper materials with few differences in properties [4,5]. Indeed, an increase in research works related to natural lignocellulosic fibers (NLFs) as reinforcement in polymeric matrices is currently observed. NLFs are already able to promote characteristics similar to composites with lower density and cost [6].

Today, most investigated and industrially used NLFs, such as jute [7–9], sisal [10–12], hemp [13–16], flax [17–19], and cotton [20–22], are considered in several applications owing

to their eco-friendly character associated with lower processing energy [23]. However, the renewability of NLFs depends on the polymer matrix as well as superficial treatments used to increase the adhesion between fiber and matrix [24].

Composites with a polymer matrix reinforced with NLFs bear considerable potential for application in automotive, furniture, packing, and armor industries [25–28]. Although those reinforced with synthetic fibers present higher mechanical performance, these composites also bear a considerable negative impact on the ecosystem, due primarily to the use of petroleum as raw material as highlighted by recent studies [29,30]. Therefore, NLFs provide a more eco-friendly character to the final material and minimize the global dependency on fossil fuels, in addition to favoring a broader range of manufacturers [31]. On the other hand, some relevant remarks must be taken into account before considering its application, such as NLF hydrophilic character, poor adhesion to the polymeric matrix [32]; non-uniform properties due to intrinsic factors such as age, extraction process, and environmental conditions [33]; low thermal stability [34]; as well as low mechanic performance compared to the synthetic fibers [35].

Kenaf fiber (*Hibiscus cannabinus* L.) is one of the most commonly used NLFs as reinforcement in polymer matrix composites and in several other industrial applications [36]. In 2020, the total harvest of kenaf crops globally yielded 126,000 tons [37]. These fibers have a significant advantage in terms of growth rate; about 3 meters in 3 months and at roughly 5 cm of thickness, even in adverse weather conditions [38]. The kenaf plant, illustrated in Figure 1a, provides distinct fibers extracted from different parts (leaves, stalks, seeds) [39], as long as sufficient care is taken during planting, growing, and harvesting [40,41]. Figure 1b illustrates the kenaf fiber surface under high magnification.

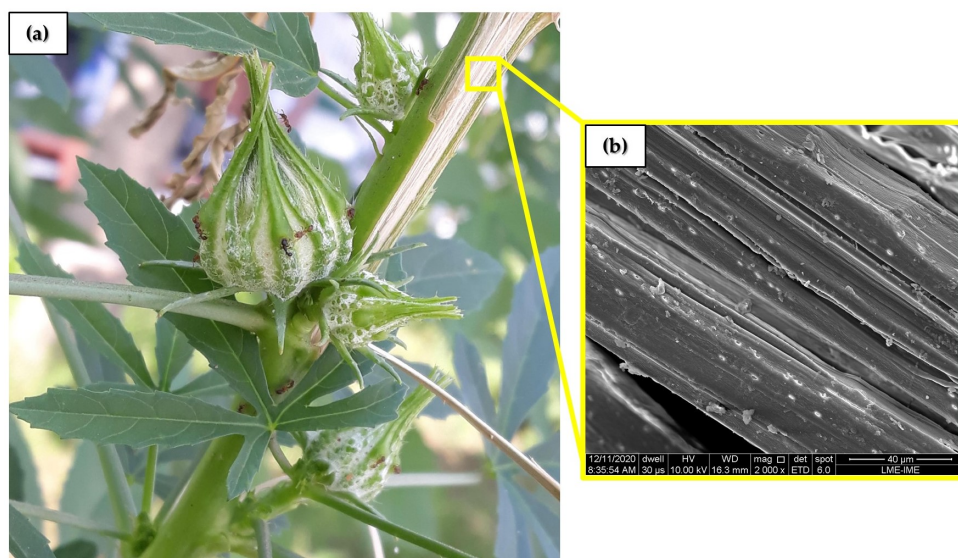


Figure 1. (a) Stem of the kenaf plant; (b) SEM of the kenaf fiber longitudinal surface.

In recent works, promising results are observed for kenaf fibers as reinforcement in different types of polymer matrices, such as HDPE [42–45], PP [46–49], polyester [50–52], epoxy [32,53–55], polylactic acid (PLA) [56–59], polystyrene [60,61], and PVC [62,63]. In particular, Ochi [64] reported an increase of 687% in tensile strength of 70 wt% kenaf fiber composites as compared to plain PLA. Many works have already highlighted the dynamic-mechanic properties of kenaf fibers [58,63,65–67]. Datta and Kopczynska [65] studied the dynamic properties, absorption and morphology of kenaf fibers treated with acetylation in a polyurethane matrix. The composites showed high damping capacity, with $\tan \delta$ less than 0.2. Woo and Cho [58] analyzed the effects of ammonium polyphosphate in the thermal and mechanical properties of a kenaf/PLA composite through dynamic-mechanical analysis (DMA). The storage module exhibited an increase of 165% in relation to unreinforced composites and the thermal and thermo-dimensional stabilities of the

biocomposites were considerably increased. Bakar et al. [63] investigated the thermal properties of a kenaf-PVC/PVA composite. With the addition of kenaf fiber, the DMA curves indicated an increase in the glass transition temperature of the composites. Saba et al. [68] studied the dynamic-mechanical properties of kenaf-epoxy filled with nano oil palm. The general results indicated that E' , E'' and T_g increased considerably with the incorporation of nanofibers from empty palm fruit bunches. Chee et al. [66] characterized the dynamic-mechanical properties of kenaf/bamboo-epoxy composites, the storage modulus of the hybrid composites before and after the glass transition region showed improvement following the addition of nanoclay. Azammi et al. [67] treated with alkalization the kenaf fibers and used them as reinforcement in natural rubber (NR) and thermoplastic polyurethane to investigate its physical, viscoelastic and dynamic-mechanical properties. In the DMA test, an increase in damping properties at high temperatures (up to 135 °C) was observed. To our knowledge, kenaf-fiber-reinforced epoxy composites have not yet been investigated for both DMA and ballistic performance. Thus, the objective of this work is to investigate for the first time, the influence of the addition of different amounts of kenaf fiber, up to 30 vol.%, on the DMA properties of epoxy composites. From the aforementioned information, it can be noted that no investigation have so far been carried out on the properties obtained from the DMA of kenaf/epoxy composites, and their ballistic performance. The worldwide cultivated and industrially applied kenaf fiber together with its superior mechanical performance as reinforcement in polymer composites were the appealing motivations to perform this research.

2. Materials and Methods

2.1. Materials

The kenaf fibers, illustrated in Figure 1, extracted from the *Hibiscus cannabinus* stalks, were supplied by the Tapete São Carlos, from São Paulo, Brazil. The as-received kenaf fibers were manually cleaned and then dried at 60 °C for 24 h, as commonly used for NLFs [69]. The fibers were not subjected to any chemical treatment. The epoxy resin used was a diglycidyl ether bisphenol A (DGEBA), hardened with triethylenetetramine (TETA) in a stoichiometric ratio of 100:13, as recommended by the manufacturer, Merck. Both resin components were supplied by Resinpoxy Ltda., Rio de Janeiro, Brazil.

2.2. Fabrication of Composites

Composite plates were produced by a compression process in a 150 × 120 mm metallic mold, 10 mm in thickness, based on ASTM D4065-01 [70], and 10, 20, and 30 vol% kenaf fibers, applying a pressure of 5 MPa for 24 h, as commonly used for NLF-based epoxy composites [16,26,71]. Aligned kenaf fibers were carefully laid inside the mold with a still fluid resin-hardener mix at a predefined proportion of fiber and resin. The epoxy resin density was considered equal to 1.11 g/cm³, the same as that found in the literature [71,72], and the fiber density was evaluated through tests, obtaining an average of 1.52 g/cm³ [71]. Figure 2 shows the specimens that were prepared for testing, according to ASTM D4065-01 [70].

2.3. Dynamic Mechanical Analysis

The DMA test was performed according to ASTM D4065-01 [70] to identify the parameters of storage modulus (E'), loss modulus (E''), and tangent delta ($\tan \delta$) obtained in the test. The equipment model Q800 (TA Instruments, New Castle, DE, USA) was used, operating at a frequency of 1 Hz, in temperatures ranging from 30 to 200 °C, with a heating rate of 3 °C/min, under a nitrogen atmosphere. The samples were subjected to the three-point bend test, where the dimensions 64 × 13 × 3 mm were used in the samples. Table 1 describes the nomenclature of the samples according to the fiber content adopted in the composite.

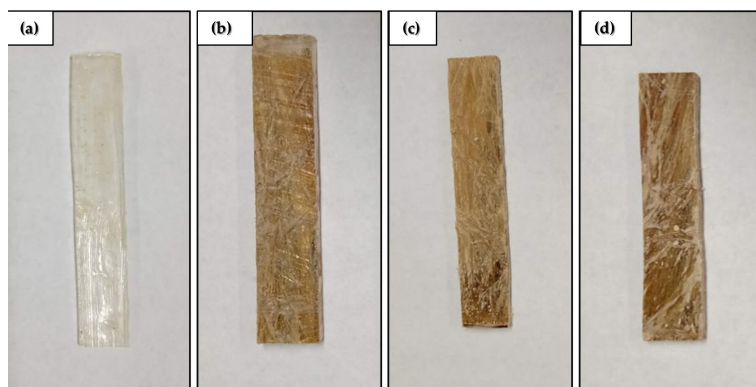


Figure 2. Samples for DMA testing: (a) epoxy resin; (b) 10 vol%, (c) 20 vol% fibers and (d) 30 vol% fibers.

Table 1. Nomenclature of the composites used in this study.

Nomenclature	Composition
EPOXY	Neat Epoxy
EK10	10 vol.% Kenaf fiber
EK20	20 vol.% Kenaf fiber
EK30	30 vol.% Kenaf fiber

2.4. Ballistic Tests

Ballistics tests were carried out in a related facility at the Military Institute of Engineering, Rio de Janeiro, Brazil. A gunpower SSS pressure rifle (Gunpower, UK) using 0.22 caliber lead ammunition with nominal 3.3 g of mass, was positioned 5 m away from the target face aligned 90 degrees (perpendicular) to the projectile trajectory, as recommended by standard NIJ 0101.06 [73]. Both impact (V_i) and residual (V_r) velocities were measured by means of two Air Chrony model MK3 ballistic chronographs, one positioned 10 cm in front and the other 10 cm behind the target, respectively. The energy absorbed by the target (E_{abs}) was calculated as [74]:

$$E_{abs} = \frac{m(V_i^2 - V_r^2)}{2} - E_{abs} \quad (1)$$

where m is the projectile mass and E_{abs} the absorbed energy during the projectile flight without target. Based on the calculated value of E_{abs} in Equation (1), an important ballistic parameter, namely the limit velocity (V_L) can be evaluated by Equation (2) [74]:

$$V_L = \sqrt{\frac{2 \cdot E_{abs}}{m}} \quad (2)$$

2.5. Scanning Electron Microscopy (SEM)

The kenaf fiber surface, as well as the kenaf–epoxy interface, were analyzed using a Quanta FEG 250 microscope, Fei (Hills-Boron, Hillsboro, OR, USA) with a secondary electron detector, an accelerating voltage of 10 kV, and a magnification ranging from 240 to 1600 \times . The fibers were covered with gold in the Leica Ace600 equipment (Wetzlar, Germany).

3. Results

3.1. Storage Modulus (E')

The storage modulus represents the elastic behavior of a material when subjected to sinusoidal stress. The storage modulus provides information about the dynamic-mechanical properties of a material, such as stiffness, load capacity, crosslink density, and interfacial strength between fiber and matrix [69,75–77]. A clear understanding of the storage module

provides important information about the stiffness, degree of crosslinking, and fiber/matrix interfacial bonding.

Figure 3 illustrates the E' curves variation with temperature for the kenaf/epoxy composites. It can be noted that the increase in temperature caused a drop in the storage modulus in all compositions. The E' results obtained are similar to those presented by Oliveira et al. [69], which produced epoxy matrix composites reinforced with thermally aged fique fabric. The curves of E' become wider in the glassy region, located between 50 and 150 °C. The increase in kenaf fiber volume fiber caused an increase in the storage modulus of all composites. The drop in curve E' starts at approximately 63 °C for EPOXY, EK20 and EK30 samples, and at 69 °C for EK10, with the drop in the curve ending in the region between 140 and 160 °C for composites EK10, EK20 and EK30, and at 120 °C for EPOXY.

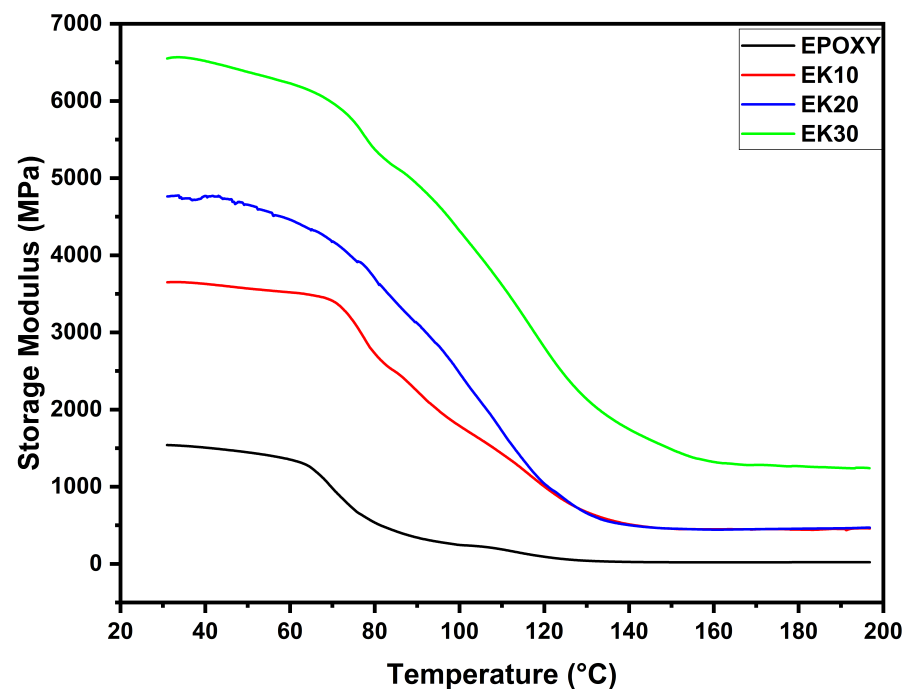


Figure 3. DMA storage modulus (E') curves for epoxy composites incorporated with different amounts of kenaf fibers.

The region where the E' drop occurs is defined as the glass transition region (T_g) of the composite, indicating the movement of the main polymeric chain [78]. Below the glass transition region, the polymeric chain movement is restricted due to the low mobility of the frozen and packed molecule arrangement. Thus, E' has a high value in the glassy state. With the increase in temperature, the arrangement of packed molecules collapses, causing the polymer chain to acquire high molecular mobility and increasing free volume components, resulting in the storage modulus dropping and moving to the viscoelastic region of the material. Table 2 shows the values of the storage module of the composites.

Table 2. Results of DMA analysis of the composites.

Composite	E' at 30 °C (MPa)	E' at 150 °C (MPa)	Peak of E'' (MPa)	Peak high of $\tan \delta$
EPOXY	1540	20	140	0.57
EK10	4760	450	390	0.30
EK20	3640	450	350	0.22
EK30	6550	1480	590	0.19

3.2. Loss Modulus (E'')

The loss modulus (E'') shows the viscous behavior of a material when subjected to an oscillating stress cycle [78]. A material with a high E'' value indicates that it has a higher energy dissipation capacity and therefore better damping properties to reduce the damaging forces caused by mechanical energy. Figure 4 shows the E'' vs. temperature curves for neat epoxy and epoxy/kenaf composites.

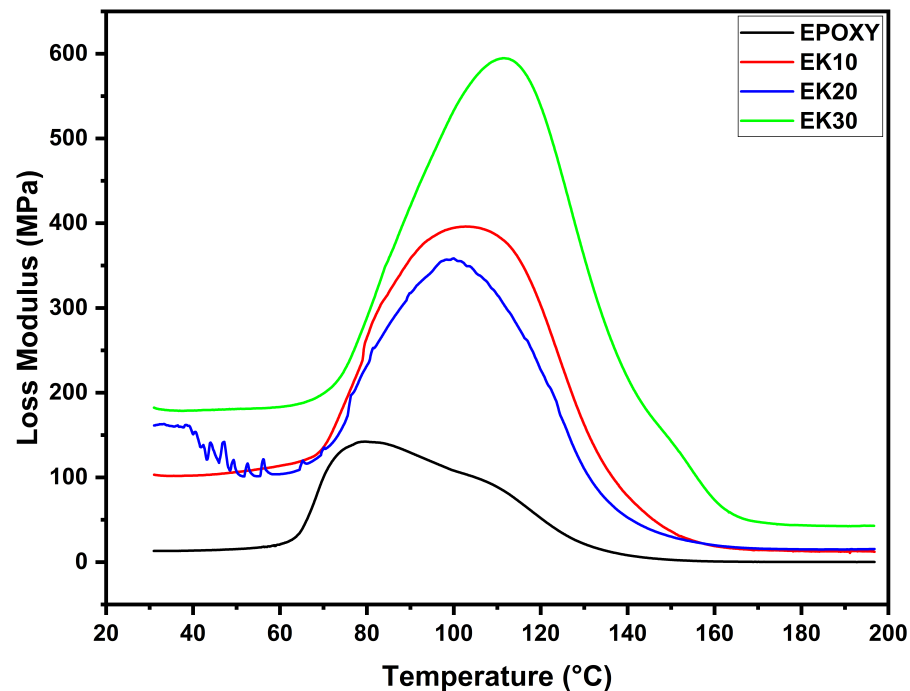


Figure 4. DMA loss modulus (E'') curves for epoxy composites incorporated with different amounts of kenaf fibers.

All composites reached a maximum peak height in the glass transition region; the values are presented in Table 2. As shown in Figure 4, the glass transition region starts at 70 °C. In this region, the loss modulus is low and constant. However, in the rubbery state the viscous behavior of the material increases. This occurs via superposition of the molecular segment motion in the polymeric chain with mechanical deformation, resulting in high internal friction and inelastic deformation [79]. This results in a high dissipation energy, with the loss modulus reaching the highest point of the peak, related to T_g of the material. After reaching this point, the polymeric molecules pass to a relaxed state and reduce their internal friction. This reduction in friction causes a drop in the loss modulus. Neat epoxy has the lowest E'' value (0.14 GPa), but with the addition of kenaf fibers an increase is observed in the loss modulus of the composites of about 178.5% for EK10, 150% for EK20, and 321.4% for EK30. The increase in kenaf fiber content as reinforcement induced greater internal friction, resulting in a higher E'' value.

3.3. Damping Factor ($\tan \delta$)

The $\tan \delta$ curve, also called loss ratio or damping factor, is obtained from the ratio between the loss modulus and storage modulus (E''/E') and is associated with the heat dissipation during each deformation cycle and an elastic behavior of the material. Thus, from Figure 5, the consequence of kenaf addition and the temperature variation on the composites damping properties can be noted. The $\tan \delta$ values of epoxy–kenaf (EK) composites (0.19–0.30) in Figure 5 are, in every case, lower than EPOXY (0.57). These results indicate that the neat epoxy presents a higher damping factor, which is related to a greater inelastic deformation with a higher energy dissipation. On the other hand, the decrease of

the peak of the EK groups can be attributed to the interlocking mechanism between the fibers and the polymer matrix, which restricts the chain movement [80]. This is visualized where the EK30 presented the lowest $\text{Tan } \delta$ peak height (0.19) in Figure 5 among the three other groups, indicating strong interfacial interaction and lower energy dissipation at the interface [81,82].

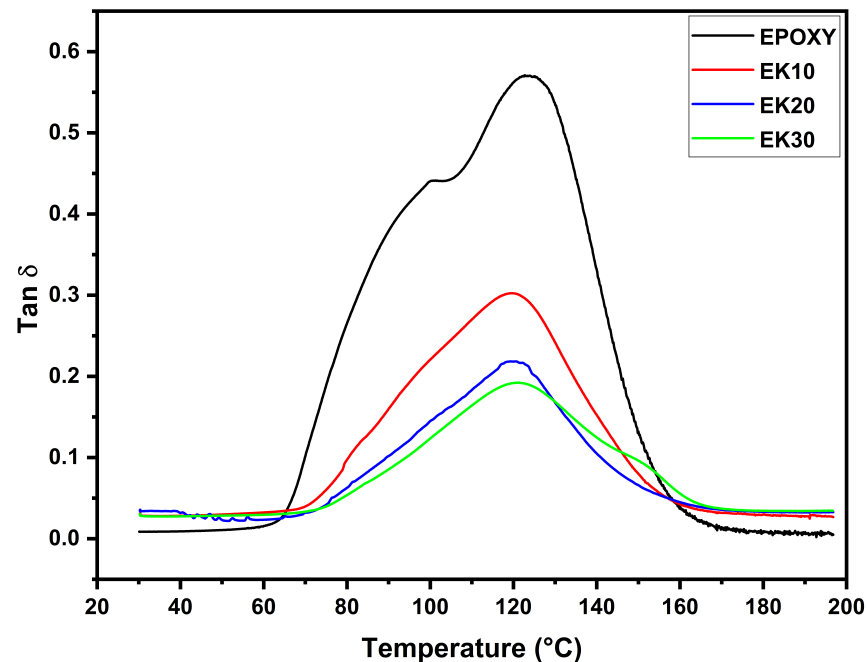


Figure 5. Damping factor ($\text{Tan } \delta$) curves for epoxy composites incorporated with different amounts of kenaf fibers.

3.4. Cole–Cole Plot

The Cole–Cole graph is obtained from the relationship between the loss modulus (E'') and the storage modulus (E') [83], from which semicircular curves for the homogeneous polymeric system [84] are obtained and related to effects present at the interface and heterogeneous dispersion of phases [85]. Thus, Figure 6 shows a regular curve for neat epoxy and a more irregular curve for EK composites, which increase for larger volumes of natural reinforcement. As aforementioned, these curves indicate a greater heterogeneous dispersion for these materials due to the presence of kenaf fibers in the polymeric structures of the resin, Figure 7 which represents a greater interfacial interaction between kenaf and epoxy in these fractions.

The results obtained are similar to the findings from previous research, in which the palm–epoxy combination in fractions of 40, 50, and 60 vol%, presented semicircular curves with greater irregularities as the reinforcement volume increased [85]. Similar behavior was also observed in the work reported by Vijayan et al. [86] for the Aloe Vera–epoxy composite.

3.5. Ballistic Test Results

The ballistic tests of ten 0.22 projectiles shot against 10 mm thick target plates with 150×120 mm of epoxy surface for both plain epoxy and 30 vol% kenaf fiber composites, resulted in corresponding impact (V_i) and residual (V_r) velocities as well as the parameters, calculated from Equations (1) and (2) and based on the NIJ 0101.06 standard [73], presented in Table 3.

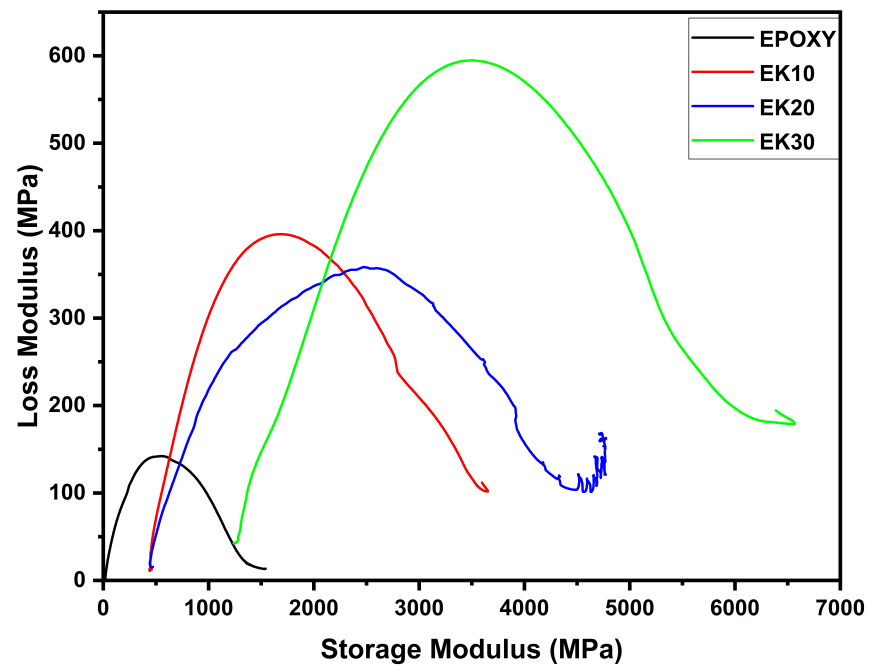


Figure 6. Cole–Cole plot for epoxy composites incorporated with different amounts of kenaf fibers.

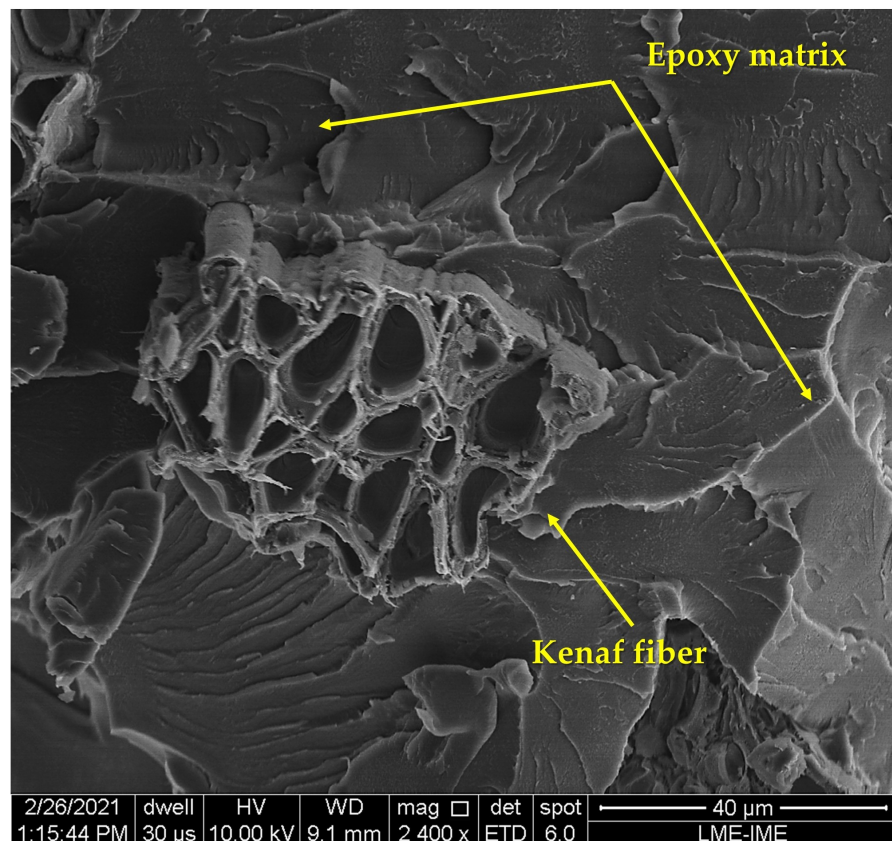


Figure 7. SEM micrograph illustrating a kenaf fiber in the epoxy matrix.

Table 3. Ballistic results of ten shots using 0.22 projectile against plain epoxy (EPOXY) and 30 vol% kenaf fiber (EK30) composite.

Target	Projectile Mass (g)	V_i (m/s)	V_r (m/s)	E_{abs} (J)	V_L (m/s)
No Target	3.11 ± 0.02	279.01 ± 13.10	275.98 ± 13.42	6.96 ± 3.62	-
Epoxy	3.10 ± 0.03	258.58 ± 36.20	158.56 ± 51.89	69.98 ± 31.69	212.48 ± 142.97
EK30	3.17 ± 0.01	288.30 ± 2.49	151.11 ± 12.01	94.81 ± 12.01	244.57 ± 87.05

To compare the ballistic absorbed energies, Figure 8 shows the values of E_{abs} from Table 3 including the corresponding error bars. Despite the greater mean value of absorber energy, for the composite, the relatively higher values of the standard deviations render them similar. The V_L of EK30 in Table 3 is superior to that reported for epoxy composites reinforced with the same 30 vol% amount of caranan and tucum fibers [87,88] as well as sedge fiber [89]. An ongoing investigation with an increased number of shootings is expected to statistically confirm the superior ballistic performance of kenaf-fiber-reinforced epoxy composites.

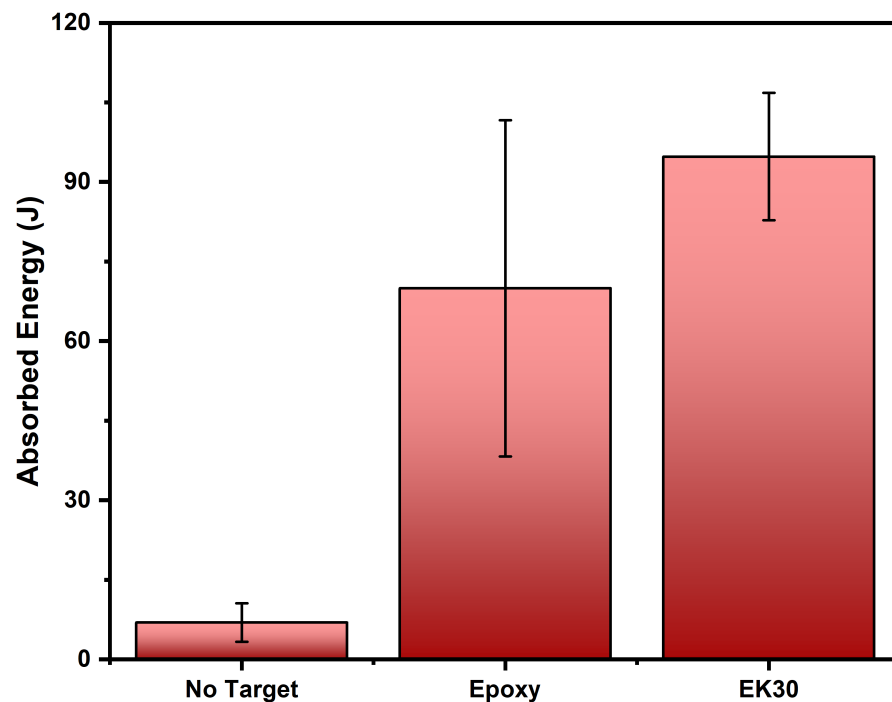


Figure 8. Values of ballistic absorbed energy against 0.22 caliber ammunition of plain epoxy, 30 vol% kenaf fiber composite and shooting condition without actual target.

3.6. Microstructure

The morphological observation of the tested samples allowed one to observe the interaction between fiber and matrix, representing a fundamental aspect regarding the mechanical properties of the material.

In Figure 9, one can observe in the fractography of the neat epoxy (Figure 9a) the high density of river marks, which indicates a brittle fracture due to the absence of reinforcement. In the micrograph of EK10 (Figure 9b), one can observe a few pulled-out fibers, which can be attributed to the low interfacial adhesion between the fiber and the polymeric matrix due to the presence of voids and cracks. As for the EK20 and EK30 composites (Figure 9c,d), they have an even greater pullout density due to an increase in the adhesion of the reinforcement to the matrix. This can be related to relevant mechanical properties with respect to the other groups. Indeed, recent ballistic results for epoxy composites

reinforced with caranan fiber [87] displayed cracks and delamination. This indicates an adhesion to the matrix less efficient than that of kenaf fiber revealed in Figures 7 and 9.

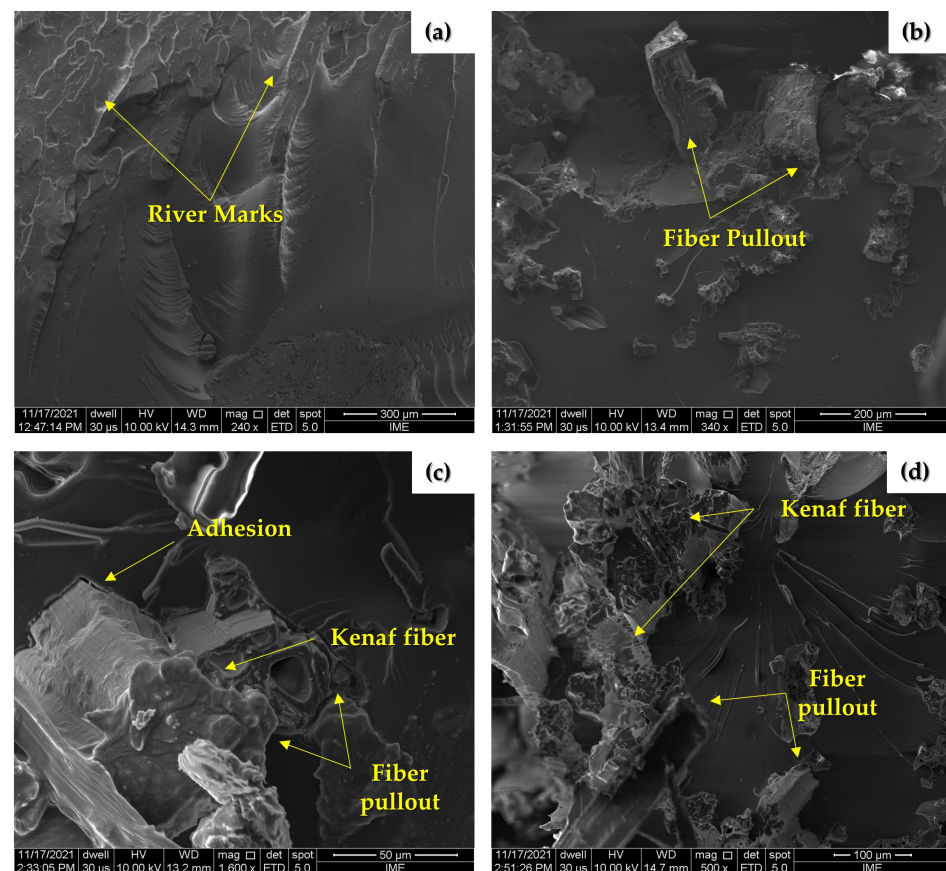


Figure 9. SEM images of fractured samples: (a) EPOXY; (b) EK10; (c) EK20; (d) EK30.

4. Summary and Conclusions

Kenaf/epoxy composites were produced in three different volumes of fibers, 0, 10, 20 and 30 vol%. From the results obtained via DMA and SEM images, the following conclusions can be made:

- i. The storage modulus (E') of every composite presented a considerable decrease at 60 °C, around the glass transition temperature, where a movement in the polymeric chains occurs and provides a rubbery state to the material.
- ii. The loss modulus (E'') of the composites increased substantially as the volume fraction of kenaf also increased.
- iii. The peaks presented on the damping factor ($\text{Tan}\delta$) graph decreased with the volume fraction of kenaf increment in the composite. This could be related to an increase of the adhesion between fiber and matrix.
- iv. In the Cole–Cole plot of the composites, a variation of the curves can be noted, specially for the neat epoxy, which appears close to a perfect semicircle. This could be associated with the lack of a second phase in the resin. The curves of the EK10, EK20, and EK30 composites presented an irregular semicircle, attributed to a greater heterogeneity of the material.
- v. Ballistic tests using 0.22 ammunition revealed similar performance in terms of absorbed energy and limit velocity for the plain epoxy and EK30 composite as targets. Despite the greater mean values for the EK30 composite, the relatively higher standard deviation remains inadequate in confirming the superior ballistic performance of the composite. A larger number of ballistic tests are required for the statistically supported determination of a definite conclusion.

- vi. The fractographies of the composites after the tests showed crack regions where the stresses propagated through the composites. In addition, an increase in the adhesion across the kenaf/epoxy interface could be observed.
- vii. The DMA and ballistic results, mainly regarding the 30 vol% kenaf-fiber-reinforced epoxy composite, confirmed not only the promising industrial applications in fields including automotive, civil construction, and furniture and packing, but also provide support for its application as a ballistic armor component.

Author Contributions: Conceptualization, methodology and investigation, T.T.d.S.; formal analysis and data curation, T.T.d.S., P.H.P.M.d.S., M.P.R. and L.d.M.N.; software, P.H.P.M.d.S. and M.P.R.; writing—original draft preparation, T.T.d.S., M.P.R., P.H.P.M.d.S. and L.d.M.N.; ballistic tests, A.B.-H.d.S.F.; special analyses, N.T.S.; writing—review and editing, L.F.C.N, F.d.C.G.F. and S.N.M.; supervision, L.F.C.N.; project administration, S.N.M. All authors have read and agreed to the published version of the manuscript.

Funding: This research work is supported by the Brazilian Agency CAPES (Coordenação de Aperfeiçoamento de Pessoal de Nível Superior), Protocol #001.

Acknowledgments: The authors would like to thank the company Tapetes São Carlos for their donation of kenaf fibers.

Conflicts of Interest: The authors declare no conflict of interest.

References

- Jaiswal, D.; Devnani, G.; Rajeshkumar, G.; Sanjay, M.; Siengchin, S. Review on extraction, characterization, surface treatment and thermal degradation analysis of new cellulosic fibers as sustainable reinforcement in polymer composites. *Curr. Res. Green Sustain. Chem.* **2022**, *5*, 100271. [[CrossRef](#)]
- Seki, Y.; Selli, F.; Erdoğan, Ü.H.; Atagür, M.; Seydibeyoğlu, M.Ö. A review on alternative raw materials for sustainable production: novel plant fibers. *Cellulose* **2022**, *29*, 4877–4918. [[CrossRef](#)]
- Pickering, K.; Efendy, M.; Le, T. A review of recent developments in natural fibre composites and their mechanical performance. *Compos. Part A Appl. Sci. Manuf.* **2016**, *83*, 98–112. [[CrossRef](#)]
- Joshi, S.V.; Drzal, L.; Mohanty, A.; Arora, S. Are natural fiber composites environmentally superior to glass fiber reinforced composites? *Compos. Part A Appl. Sci. Manuf.* **2004**, *35*, 371–376. [[CrossRef](#)]
- Balla, V.K.; Kate, K.H.; Satyavolu, J.; Singh, P.; Tadimetri, J.G.D. Additive manufacturing of natural fiber reinforced polymer composites: Processing and prospects. *Compos. Part B Eng.* **2019**, *174*, 106956. [[CrossRef](#)]
- Neto, J.; Queiroz, H.; Aguiar, R.; Lima, R.; Cavalcanti, D.; Banea, M.D. A Review of Recent Advances in Hybrid Natural Fiber Reinforced Polymer Composites. *J. Renew. Mater.* **2022**, *10*, 561. [[CrossRef](#)]
- Chaturvedi, R.; Pappu, A.; Tyagi, P.; Patidar, R.; Khan, A.; Mishra, A.; Gupta, M.K.; Thakur, V.K. Next-generation high-performance sustainable hybrid composite materials from silica-rich granite waste particulates and jute textile fibres in epoxy resin. *Ind. Crop. Prod.* **2022**, *177*, 114527. [[CrossRef](#)]
- Shenoy Heckadka, S.; Pai Ballambat, R.; Kini Manjeshwar, V.; Kumar, M.; Hegde, P.; Kamath, A. Damage Characterization of Ultra High Molecular Weight Polyethylene/Flax/Jute Fiber Reinforced Melamine Formaldehyde Hybrid Composites using Cone Beam Computed Tomography. *Nondestruct. Test. Eval.* **2022**, *37*, 400–426. [[CrossRef](#)]
- Van Cong, D.; Giang, N.V.; Trung, T.H.; Hoang, T.; Lam, T.D.; Tham, D.Q.; Huong, N.T. Biocomposites from polyamide 11 reinforced by organic silane modified jute fibers: Fabrication and characterization. *J. Appl. Polym. Sci.* **2022**, *139*, 51795. [[CrossRef](#)]
- Pantano, A.; Militello, C.; Bongiorno, F.; Zuccarello, B. Analysis of the Parameters Affecting the Stiffness of Short Sisal Fiber Biocomposites Manufactured by Compression-Molding. *Polymers* **2022**, *14*, 154. [[CrossRef](#)]
- Loganathan, T.M.; Naveen, J.; Reshwanth, K.N.G.L.; Jayakrishna, K.; Muthukumar, C. Thermal Properties of Sisal Fiber-Based Hybrid Composites. In *Natural Fiber-Reinforced Composites: Thermal Properties and Applications*; Wiley: New York, NY, USA, 2022; pp. 85–92.
- Makunza, J.K.; Kumaran, G.S. An Experimental Investigation on Suitability of Using Sisal Fibers in Reinforced Concrete Composites. In *Proceedings of the Construction Technologies and Architecture, 2022; Volume 1*, pp. 24–34.
- da Silveira, P.H.P.; Ribeiro, M.P.; Silva, T.T.; Lima, A.M.; Lemos, M.F.; Oliveira, A.G.; Nascimento, L.F.C.; Gomes, A.V.; Monteiro, S.N. Effect of Alkaline Treatment and Graphene Oxide Coating on Thermal and Chemical Properties of Hemp (*Cannabis sativa* L.) Fibers. *J. Nat. Fibers* **2022**, 1–14. [[CrossRef](#)]
- Dhakal, H.N.; Sain, M. Thermal Properties of Hemp Fiber-Based Hybrid Composites. In *Natural Fiber-Reinforced Composites: Thermal Properties and Applications*; Wiley: New York, NY, USA, 2022; pp. 183–200.
- Dolça, C.; Fages, E.; Gonga, E.; Garcia-Sanoguera, D.; Balart, R.; Quiles-Carrillo, L. The Effect of Varying the Amount of Short Hemp Fibers on Mechanical and Thermal Properties of Wood–Plastic Composites from Biobased Polyethylene Processed by Injection Molding. *Polymers* **2022**, *14*, 138. [[CrossRef](#)] [[PubMed](#)]

16. Ribeiro, M.P.; de Mendonça Neuba, L.; da Silveira, P.H.P.M.; da Luz, F.S.; da Silva Figueiredo, A.B.H.; Monteiro, S.N.; Moreira, M.O. Mechanical, thermal and ballistic performance of epoxy composites reinforced with Cannabis sativa hemp fabric. *J. Mater. Res. Technol.* **2021**, *12*, 221–233. [[CrossRef](#)]
17. Malik, K.; Ahmad, F.; Yunus, N.A.; Gunister, E.; Nakato, T.; Mouri, E.; Ali, S. A Review of Flax Fiber Reinforced Thermoset Polymer Composites: Thermal-Physical Properties, Improvements and Application. *J. Nat. Fibers* **2021**, 1–19. [[CrossRef](#)]
18. Santulli, C. Thermal Properties of Flax Fiber Hybrid Composites. In *Natural Fiber-Reinforced Composites: Thermal Properties and Applications*; Wiley: New York, NY, USA, 2022; pp. 93–105.
19. Giuliani, P.M.; Giannini, O.; Panciroli, R. Characterizing flax fiber reinforced bio-composites under monotonic and cyclic tensile loading. *Compos. Struct.* **2022**, *280*, 114803. [[CrossRef](#)]
20. Cao, W.; Li, Q.; Wu, C. The HDPE composites reinforced with waste hybrid PET/cotton fibers modified with the synthesized modifier. *e-Polymers* **2022**, *22*, 30–37. [[CrossRef](#)]
21. Gama, N.; Godinho, B.; Barros-Timmons, A.; Ferreira, A. PU composites based on different types of textile fibers. *J. Compos. Mater.* **2021**, *55*, 3615–3626. [[CrossRef](#)]
22. Azmami, O.; Sajid, L.; Boukhriess, A.; Majid, S.; El Ahmadi, Z.; Benayada, A.; Gmouh, S. Mechanical and aging performances of Palm/Wool and Palm/Polyester nonwovens coated by waterborne polyurethane for automotive interiors. *Ind. Crop. Prod.* **2021**, *170*, 113681. [[CrossRef](#)]
23. Latif, R.; Wakeel, S.; Zaman Khan, N.; Noor Siddiquee, A.; Lal Verma, S.; Akhtar Khan, Z. Surface treatments of plant fibers and their effects on mechanical properties of fiber-reinforced composites: A review. *J. Reinf. Plast. Compos.* **2019**, *38*, 15–30. [[CrossRef](#)]
24. del Campo, A.S.M.; Robledo-Ortiz, J.R.; Arellano, M.; Rabelero, M.; Pérez-Fonseca, A.A. Accelerated weathering of polylactic acid/agave fiber biocomposites and the effect of fiber–matrix adhesion. *J. Polym. Environ.* **2021**, *29*, 937–947. [[CrossRef](#)]
25. Sathish, S.; Prabhu, L.; Gokulkumar, S.; Karthi, N.; Balaji, D.; Vigneshkumar, N. Extraction, Treatment and Applications of Natural Fibers for Bio-Composites—A Critical Review. *Int. Polym. Process.* **2021**, *36*, 114–130. [[CrossRef](#)]
26. Garcia Filho, F.C.; Luz, F.S.; Oliveira, M.S.; Bezerra, W.; Barbosa, J.D.; Monteiro, S.N. Influence of Rigid Brazilian Natural Fiber Arrangements in Polymer Composites: Energy Absorption and Ballistic Efficiency. *J. Compos. Sci.* **2021**, *5*, 201. [[CrossRef](#)]
27. Khalid, M.Y.; Imran, R.; Arif, Z.U.; Akram, N.; Arshad, H.; Rashid, A.A.; García Márquez, F.P. Developments in Chemical Treatments, Manufacturing Techniques and Potential Applications of Natural-Fibers-Based Biodegradable Composites. *Coatings* **2021**, *11*, 293. [[CrossRef](#)]
28. Ilyas, R.; Sapuan, S.; Nurazzi, N.M.; Norraahim, M.N.F.; Ibrahim, R.; Atikah, M.; Huzaifah, M.; Radzi, A.; Izwan, S.; Azammi, A.N.; et al. Macro to nanoscale natural fiber composites for automotive components: Research, development, and application. In *Biocomposite and Synthetic Composites for Automotive Applications*; Wiley: New York, NY, USA, 2021; pp. 51–105.
29. Yang, J.; Ching, Y.C.; Chuah, C.H. Applications of lignocellulosic fibers and lignin in bioplastics: A review. *Polymers* **2019**, *11*, 751. [[CrossRef](#)] [[PubMed](#)]
30. Choo, K.; Ching, Y.C.; Chuah, C.H.; Julai, S.; Liou, N.S. Preparation and characterization of polyvinyl alcohol-chitosan composite films reinforced with cellulose nanofiber. *Materials* **2016**, *9*, 644. [[CrossRef](#)]
31. Tan, B.K.; Ching, Y.C.; Poh, S.C.; Abdullah, L.C.; Gan, S.N. A review of natural fiber reinforced poly (vinyl alcohol) based composites: Application and opportunity. *Polymers* **2015**, *7*, 2205–2222. [[CrossRef](#)]
32. Suriani, M.; Zainudin, H.A.; Ilyas, R.; Petru, M.; Sapuan, S.; Ruzaidi, C.; Mustapha, R. Kenaf Fiber/Pet Yarn Reinforced Epoxy Hybrid Polymer Composites: Morphological, Tensile, and Flammability Properties. *Polymers* **2021**, *13*, 1532. [[CrossRef](#)]
33. Monteiro, S.N.; Lopes, F.P.D.; Barbosa, A.P.; Bevitore, A.B.; Da Silva, I.L.A.; Da Costa, L.L. Natural lignocellulosic fibers as engineering materials—an overview. *Metall. Mater. Trans. A* **2011**, *42*, 2963–2974. [[CrossRef](#)]
34. Priya, B.; Gupta, V.K.; Pathania, D.; Singha, A.S. Synthesis, characterization and antibacterial activity of biodegradable starch/PVA composite films reinforced with cellulosic fibre. *Carbohydr. Polym.* **2014**, *109*, 171–179. [[CrossRef](#)]
35. Zhao, X.; Copenhaver, K.; Wang, L.; Korey, M.; Gardner, D.J.; Li, K.; Lamm, M.E.; Kishore, V.; Bhagia, S.; Tajvidi, M.; et al. Recycling of natural fiber composites: Challenges and opportunities. *Resour. Conserv. Recycl.* **2022**, *177*, 105962. [[CrossRef](#)]
36. Karnani, R.; Krishnan, M.; Narayan, R. Biofiber-reinforced polypropylene composites. *Polym. Eng. Sci.* **1997**, *37*, 476–483. [[CrossRef](#)]
37. Harussani, M.; Sapuan, S. Development of Kenaf biochar in engineering and agricultural applications. *Chem. Afr.* **2022**, *5*, 1–17. [[CrossRef](#)]
38. Aziz, S.H.; Ansell, M.P.; Clarke, S.J.; Panteny, S.R. Modified polyester resins for natural fibre composites. *Compos. Sci. Technol.* **2005**, *65*, 525–535. [[CrossRef](#)]
39. Ramesh, M. Kenaf (*Hibiscus cannabinus* L.) fibre based bio-materials: A review on processing and properties. *Prog. Mater. Sci.* **2016**, *78*, 1–92. [[CrossRef](#)]
40. Meints, P.D.; Smith, C. Kenaf seed storage duration on germination, emergence, and yield. *Ind. Crop. Prod.* **2003**, *17*, 9–14. [[CrossRef](#)]
41. Manzanares, M.; Tenorio, J.; Ayerbe, L. Sowing time, cultivar, plant population and application of N fertilizer on Kenaf in Spain’s central plateau. *Biomass Bioenergy* **1997**, *12*, 263–271. [[CrossRef](#)]
42. Salleh, F.M.; Hassan, A.; Yahya, R.; Azzahari, A.D. Effects of extrusion temperature on the rheological, dynamic mechanical and tensile properties of kenaf fiber/HDPE composites. *Compos. Part B Eng.* **2014**, *58*, 259–266. [[CrossRef](#)]

43. Aji, I.; Zainudin, E.; Sapuan, S.; Khalina, A.; Khairul, M. Study of hybridized kenaf/palp-reinforced HDPE composites by dynamic mechanical analysis. *Polym.-Plast. Technol. Eng.* **2012**, *51*, 146–153. [[CrossRef](#)]
44. Tewari, R.; Singh, M.K.; Zafar, S.; Powar, S. Parametric optimization of laser drilling of microwave-processed kenaf/HDPE composite. *Polym. Polym. Compos.* **2021**, *29*, 176–187. [[CrossRef](#)]
45. Singh, M.K.; Zafar, S. Wettability, absorption and degradation behavior of microwave-assisted compression molded kenaf/HDPE composite tank under various environments. *Polym. Degrad. Stab.* **2021**, *185*, 109500. [[CrossRef](#)]
46. Rahim, N.A.A.; Xian, L.Y.; Munusamy, Y.; Zakaria, Z.; Ramarad, S. Melt behavior of polypropylene-co-ethylene composites filled with dual component of sago and kenaf natural filler. *J. Appl. Polym. Sci.* **2022**, *139*, 51621. [[CrossRef](#)]
47. Irfan, M.S.; Umer, R.; Rao, S. Optimization of Compounding Parameters for Extrusion to Enhance Mechanical Performance of Kenaf-Polypropylene Composites. *Fibers Polym.* **2021**, *22*, 1378–1387. [[CrossRef](#)]
48. Sabaruddin, F.A.; Paridah, M.; Sapuan, S.; Ilyas, R.; Lee, S.H.; Abdan, K.; Mazlan, N.; Roseley, A.S.M.; Abdul Khalil, H. The effects of unbleached and bleached nanocellulose on the thermal and flammability of polypropylene-reinforced kenaf core hybrid polymer bionanocomposites. *Polymers* **2021**, *13*, 116. [[CrossRef](#)]
49. Anggraini, L.; Anjany, A. Sustainable Fabrication Technology of Composite Board by Kenaf-Polypropylene for Automobile Door Interior Applications. *Proc. Key Eng. Mater.* **2021**, *897*, 51–56. [[CrossRef](#)]
50. Arjmandi, R.; Yildirim, I.; Hatton, F.; Hassan, A.; Jefferies, C.; Mohamad, Z.; Othman, N. Kenaf fibers reinforced unsaturated polyester composites: A review. *J. Eng. Fibers Fabr.* **2021**, *16*, 15589250211040184. [[CrossRef](#)]
51. Ornaghi, H.L.; Neves, R.M.; Monticeli, F.M.; Thomas, S. Modeling of dynamic mechanical curves of kenaf/polyester composites using surface response methodology. *J. Appl. Polym. Sci.* **2021**, *139*, 52078. [[CrossRef](#)]
52. Razavi, M.; Ogunbode, E.B.; Nyakuma, B.B.; Razavi, M.; Yatim, J.M.; Lawal, T.A. Fabrication, characterisation and durability performance of kenaf fibre reinforced epoxy, vinyl and polyester-based polymer composites. *Biomass Convers. Biorefinery* **2021**, 1–16. [[CrossRef](#)]
53. Rangaraj, R.; Sathish, S.; Mansadevi, T.; Supriya, R.; Surakasi, R.; Aravindh, M.; Karthick, A.; Mohanavel, V.; Ravichandran, M.; Muhibbullah, M.; et al. Investigation of Weight Fraction and Alkaline Treatment on Catechu Linnaeus/Hibiscus cannabinus/Sansevieria Ehrenbergii Plant Fibers-Reinforced Epoxy Hybrid Composites. *Adv. Mater. Sci. Eng.* **2022**, *2022*, 4940531. [[CrossRef](#)]
54. Hammami, H.; Jawaaid, M.; Kallel, A. Effects of oil palm and montmorillonite nanofillers on stiffness and interfacial adhesion of kenaf/epoxy hybrid nanocomposites. *Polym. Compos.* **2021**, *42*, 2948–2957. [[CrossRef](#)]
55. Sapiai, N.; Jumahat, A.; Shaari, N.; Tahir, A. Mechanical properties of nanoclay-filled kenaf and hybrid glass/kenaf fiber composites. *Mater. Today Proc.* **2021**, *46*, 1787–1791. [[CrossRef](#)]
56. Azlin, M.; Sapuan, S.; Zuhri, M.; Zainudin, E. Effect of Stacking Sequence and Fiber Content on Mechanical and Morphological Properties of Woven Kenaf/Polyester Fiber Reinforced Poly(lactic acid) (PLA) Hybrid Laminated Composites. *J. Mater. Res. Technol.* **2021**, *16*, 1190–1201. [[CrossRef](#)]
57. Alias, N.F.; Ismail, H.; Ishak, K.M.K. Poly (lactic acid)/natural rubber/kenaf biocomposites production using poly (methyl methacrylate) and epoxidized natural rubber as co-compatibilizers. *Iran. Polym. J.* **2021**, *30*, 737–749. [[CrossRef](#)]
58. Woo, Y.; Cho, D. Effects of Ammonium Polyphosphate on the Flame Retarding, Tensile, Dynamic Mechanical, and Thermal Properties of Kenaf Fiber/Poly (lactic acid) Biocomposites Fabricated by Compression Molding. *Fibers Polym.* **2021**, *22*, 1388–1396. [[CrossRef](#)]
59. Haryati, A.; Razali, N.; Petr, M.; Taha, M.; Muhammad, N.; Ilyas, R.A. Effect of Chemically Treated Kenaf Fibre on Mechanical and Thermal Properties of PLA Composites Prepared through Fused Deposition Modeling (FDM). *Polymers* **2021**, *13*, 3299.
60. Zi Mun, C.; Kwong, K.Z.; Lee, F.W.; Lim, J.H. Mechanical, sound and thermal properties of recycled expanded polystyrene concrete reinforced with 0.5% to 5.5% kenaf fibre. *Eur. J. Environ. Civ. Eng.* **2021**, 1–14. [[CrossRef](#)]
61. Moustafa, H.; El-Wakil, A.E.A.A.; Nour, M.T.; Youssef, A.M. Kenaf fibre treatment and its impact on the static, dynamic, hydrophobicity and barrier properties of sustainable polystyrene biocomposites. *RSC Adv.* **2020**, *10*, 29296–29305. [[CrossRef](#)]
62. Bakar, N.; Chee, C.Y.; Abdullah, L.C.; Ratnam, C.T.; Azowa, N. Effect of methyl methacrylate grafted kenaf on mechanical properties of polyvinyl chloride/ethylene vinyl acetate composites. *Compos. Part A Appl. Sci. Manuf.* **2014**, *63*, 45–50. [[CrossRef](#)]
63. Bakar, N.A.; Chee, C.Y.; Abdullah, L.C.; Ratnam, C.T.; Ibrahim, N.A. Thermal and dynamic mechanical properties of grafted kenaf filled poly (vinyl chloride)/ethylene vinyl acetate composites. *Mater. Des. (1980–2015)* **2015**, *65*, 204–211. [[CrossRef](#)]
64. Ochi, S. Mechanical properties of kenaf fibers and kenaf/PLA composites. *Mech. Mater.* **2008**, *40*, 446–452. [[CrossRef](#)]
65. Datta, J.; Kopczyńska, P. Effect of kenaf fibre modification on morphology and mechanical properties of thermoplastic polyurethane materials. *Ind. Crop. Prod.* **2015**, *74*, 566–576. [[CrossRef](#)]
66. Chee, S.S.; Jawaaid, M.; Alothman, O.Y.; Fouad, H. Effects of nanoclay on mechanical and dynamic mechanical properties of bamboo/kenaf reinforced epoxy hybrid composites. *Polymers* **2021**, *13*, 395. [[CrossRef](#)] [[PubMed](#)]
67. Azammi, A.N.; Sapuan, S.; Ishak, M.R.; Sultan, M.T. Physical and damping properties of kenaf fibre filled natural rubber/thermoplastic polyurethane composites. *Def. Technol.* **2020**, *16*, 29–34. [[CrossRef](#)]
68. Saba, N.; Paridah, M.; Abdan, K.; Ibrahim, N.A. Dynamic mechanical properties of oil palm nano filler/kenaf/epoxy hybrid nanocomposites. *Constr. Build. Mater.* **2016**, *124*, 133–138. [[CrossRef](#)]

69. Oliveira, M.S.; da Luz, F.S.; da Costa Garcia Filho, F.; Pereira, A.C.; de Oliveira Aguiar, V.; Lopera, H.A.C.; Monteiro, S.N. Dynamic Mechanical Analysis of Thermally Aged Fique Fabric-Reinforced Epoxy Composites. *Polymers* **2021**, *13*, 4037. [[CrossRef](#)] [[PubMed](#)]
70. ASTM 4065; American Society For Testing Materials. ASTM: West Conshohocken, PA, USA, 2020.
71. Silva, T.T.d.; Silveira, P.H.P.M.d.; Ribeiro, M.P.; Lemos, M.F.; da Silva, A.P.; Monteiro, S.N.; Nascimento, L.F.C. Thermal and Chemical Characterization of Kenaf Fiber (*Hibiscus cannabinus*) Reinforced Epoxy Matrix Composites. *Polymers* **2021**, *13*, 2016. [[CrossRef](#)]
72. Kerche, E.F.; da Silva, V.D.; Fonseca, E.; Salles, N.A.; Schrekker, H.S.; Amico, S.C. Epoxy-based composites reinforced with imidazolium ionic liquid-treated aramid pulp. *Polymer* **2021**, *226*, 123787. [[CrossRef](#)]
73. NIJ 0101.04; Ballistic Resistance of Personal Body Armor, NIJ Standard-0101.04. National Institute of Justice: Washington, DC, USA, 2008.
74. Morye, S.; Hine, P.; Duckett, R.; Carr, D.; Ward, I. Modelling of the energy absorption by polymer composites upon ballistic impact. *Compos. Sci. Technol.* **2000**, *60*, 2631–2642. [[CrossRef](#)]
75. Sand Chee, S.; Jawaid, M. The effect of Bi-functionalized MMT on morphology, thermal stability, dynamic mechanical, and tensile properties of epoxy/organoclay nanocomposites. *Polymers* **2019**, *11*, 2012. [[CrossRef](#)]
76. Miyagawa, H.; Misra, M.; Drzal, L.T.; Mohanty, A.K. Novel biobased nanocomposites from functionalized vegetable oil and organically-modified layered silicate clay. *Polymer* **2005**, *46*, 445–453. [[CrossRef](#)]
77. Joseph, S.; Appukuttan, S.P.; Kenny, J.M.; Puglia, D.; Thomas, S.; Joseph, K. Dynamic mechanical properties of oil palm microfibril-reinforced natural rubber composites. *J. Appl. Polym. Sci.* **2010**, *117*, 1298–1308. [[CrossRef](#)]
78. Luz, F.S.d.; Monteiro, S.N.; Tommasini, F.J. Evaluation of dynamic mechanical properties of PALF and coir fiber reinforcing epoxy composites. *Mater. Res.* **2018**, *21*. [[CrossRef](#)]
79. Jesuarockiam, N.; Jawaid, M.; Zainudin, E.S.; Thariq Hameed Sultan, M.; Yahaya, R. Enhanced thermal and dynamic mechanical properties of synthetic/natural hybrid composites with graphene nanoplatelets. *Polymers* **2019**, *11*, 1085. [[CrossRef](#)] [[PubMed](#)]
80. Hazarika, A.; Mandal, M.; Maji, T.K. Dynamic mechanical analysis, biodegradability and thermal stability of wood polymer nanocomposites. *Compos. Part B Eng.* **2014**, *60*, 568–576. [[CrossRef](#)]
81. Naveen, J.; Jawaid, M.; Zainudin, E.; Sultan, M.T.; Yahaya, R.; Majid, M.A. Thermal degradation and viscoelastic properties of Kevlar/Cocos nucifera sheath reinforced epoxy hybrid composites. *Compos. Struct.* **2019**, *219*, 194–202. [[CrossRef](#)]
82. Yoon, O.J.; Jung, C.Y.; Sohn, I.Y.; Kim, H.J.; Hong, B.; Jhon, M.S.; Lee, N.E. Nanocomposite nanofibers of poly (D, L-lactic-co-glycolic acid) and graphene oxide nanosheets. *Compos. Part A Appl. Sci. Manuf.* **2011**, *42*, 1978–1984. [[CrossRef](#)]
83. Devi, L.U.; Bhagawan, S.; Thomas, S. Dynamic mechanical analysis of pineapple leaf/glass hybrid fiber reinforced polyester composites. *Polym. Compos.* **2010**, *31*, 956–965. [[CrossRef](#)]
84. Joshi, M.; Butola, B. a. George Simon and N. Kukaleva. *Macromolecules* **2006**, *39*, 1839–1849. [[CrossRef](#)]
85. Gheith, M.H.; Aziz, M.A.; Ghori, W.; Saba, N.; Asim, M.; Jawaid, M.; Alothman, O.Y. Flexural, thermal and dynamic mechanical properties of date palm fibres reinforced epoxy composites. *J. Mater. Res. Technol.* **2019**, *8*, 853–860. [[CrossRef](#)]
86. Vijayan, R.; Rathinasuriyan, C.; Palanisamy, R.; Geetha T., T. Viscoelastic behavior of natural fiber reinforced composite material. *Mater. Today Proc.* **2021**, *52*, 1942–1945.
87. Souza, A.T.; Neuba, L.d.M.; Junio, R.F.P.; Carvalho, M.T.; Candido, V.S.; Figueiredo, A.B.H.d.S.; Monteiro, S.N.; Nascimento, L.F.C.; da Silva, A.C.R. Ballistic Properties and Izod Impact Resistance of Novel Epoxy Composites Reinforced with Caranán Fiber (*Mauritiella armata*). *Polymers* **2022**, *14*, 3348. [[CrossRef](#)]
88. Oliveira, M.S.; Luz, F.S.d.; Teixeira Souza, A.; Demosthenes, L.C.d.C.; Pereira, A.C.; Filho, F.d.C.G.; Braga, F.d.O.; Figueiredo, A.B.H.d.S.; Monteiro, S.N. Tucum fiber from Amazon *Astrocaryum vulgare* palm tree: Novel reinforcement for polymer composites. *Polymers* **2020**, *12*, 2259. [[CrossRef](#)] [[PubMed](#)]
89. de Mendonça Neuba, L.; Pereira Junio, R.F.; Ribeiro, M.P.; Souza, A.T.; de Sousa Lima, E.; Garcia Filho, F.d.C.; Figueiredo, A.B.H.d.S.; Braga, F.d.O.; Azevedo, A.R.G.d.; Monteiro, S.N. Promising mechanical, thermal, and ballistic properties of novel epoxy composites reinforced with *Cyperus malaccensis* sedge fiber. *Polymers* **2020**, *12*, 1776. [[CrossRef](#)] [[PubMed](#)]